

The Effect of AGN and SNe Feedback on Star Formation, Reionization and the Near Infrared Background

Lei Wang¹, Ji-Rong Mao², Shou-Ping Xiang¹ and Ye-Fei Yuan¹

¹ Center for Astrophysics, University of Science and Technology of China, Hefei 230026, China
wsl2008@mail.ustc.edu.cn

² Yunnan Observatory, National Astronomical Observatories, Chinese Academy of Sciences, Kunming 650011, China

Received 2007 December 15; accepted 2008 May 16

Abstract Feedback from supernovae (SNe) and from active galactic nuclei (AGN) accompanies the history of star formation and galaxy evolution. We present an analytic model to explain how and when the SNe and AGN exert their feedback effects on the star formation and galaxy evolution processes. By using SNe and AGN kinetic feedback mechanisms based on the Lambda Cold Dark Matter (LCDM) model, we explore how these feedback mechanisms affect the star formation history (SFH), the Near-Infrared Background (NIRB) flux and the cosmological reionization. We find the values of the feedback strengths, $\epsilon_{\text{AGN}} = 1.0^{+0.5}_{-0.3}$ and $\epsilon_{\text{SN}} = 0.04^{+0.02}_{-0.02}$, can provide a reasonable explanation of most of the observational results, and that the AGN feedback effect on star formation history is quite different from the SNe feedback at high redshifts. Our conclusions manifest quantitatively that these feedback effects decrease star formation rate density (SFRD) and the NIRB flux (in $1.4 - 4.0 \mu\text{m}$), and postpone the time of completion of the cosmological reionization.

Key words: cosmology: theory – galaxies: evolution – infrared: general – stars: formation

1 INTRODUCTION

In the past few years, the Lambda Cold Dark Matter (LCDM) cosmological model and the so-called “bottom-up” hierarchical theory for large-scale structure formation have obtained decisive support from various observational data and high-resolution numerical simulations (e.g., N-body, hydrodynamics). However, many questions are still open on the details of the evolution of cosmic baryons. For example, how and when does the feedback from SNe explosions and AGN activity affect the star formation history (SFH) and the reionization history of the intergalactic medium (IGM)? In our opinion, the complexity of the interaction between star evolution and their feedback effect should be partly responsible for these uncertainties.

On the other hand, ongoing observations of the WMAP satellite on Cosmic Microwave Background (CMB) and the highest redshift QSOs put tight constraints on the reionization history of the universe. Recent detections of the Gunn-Peterson trough in the spectra of QSOs with $z \simeq 6$ indicate less than 50% neutral hydrogen at $z \sim 6.5$ (Gunn & Peterson 1965; Wyithe et al. 2005; Fan et al. 2006). The CMB observation (WMAP 3 year data) manifests that the Thomson electron scattering optical depth, $\tau_e = 0.09^{+0.03}_{-0.03}$ (Spergel et al. 2007), which suggests that our universe might be reionized during the period of redshift $7 \leq z_{\text{re}} \leq 12$ ($z_{\text{re}} = 11$ is the recommended value by the group). Another problem about cosmic baryons arises from the observed excessive emission of Near-Infrared Background (NIRB) light. Based on the observational data obtained by the Infrared Telescope in Space (IRTS), it is found that a significant isotropic

excessive emission exists in the wavelength bands from 1.4 to 4.0 μm (Matsumoto et al. 2005). Such an excessive emission of NIRB implies that there are some unknown ingredients in the extragalactic background light.

The feedback kinetic energy carried by winds and shocks can heat cold gas to hot phase through the electron-impact excitation mechanism. For lack of the raw material (condensed cold gas) the star formation (SF) is suppressed or even quenched (Granato et al. 2004). Therefore, the reionization and the NIRB are also strongly affected by the feedback process. In this paper we focus on the effects of kinetic feedback on the SFH, the cosmological reionization history and the NIRB. Two major feedback effects, the SNe feedback and the AGN feedback, are taken into account.

The outline of this paper is as follows. In Section 2 we adopt an analytic model to deal with the SF process and feedback effects. We use the ‘‘Starburst99’’¹ program to determine some of the parameters and the galaxy spectra. In Section 3 we discuss the effects of AGN and SNe feedback on NIRB. Cosmological reionization with feedback process is studied in Section 4. Finally, our discussion on some model parameters and our conclusions are presented in the last two sections. In this paper we adopt the cosmological parameters consistent with the 3 year WMAP data ($\Omega = 1.0$, $\Omega_m = 0.24$, $\Omega_\Lambda = 0.76$, $\Omega_b = 0.044$, $h = 0.72$ and $\sigma_8 = 0.76$).

2 ANALYTIC MODEL OF STAR FORMATION AND FEEDBACK

2.1 Redshift Evolution of SF

It is well-known that we are likely to be living in a Cold Dark Matter universe with a non-zero cosmological constant. According to the cosmological theory, the large-scale structure formation in such an LCDM universe is in accordance with the hierarchical scenario, in which galaxies and other luminous objects are assumed to form through baryonic gas cooling and condensation within Dark Matter (DM) halos (White & Rees 1978). Accurate analytic formulae are now available for many properties of the dark halo population in such a universe. Here, we use the modified Press-Schechter (PS, Press & Schechter 1974) formalism of Sasaki (1994) to study the halos evolution (see also Chiu & Ostriker 2000; Choudhury & Srianand 2002). In this formalism the number density of collapsed objects with mass in the range $(M, M + dM)$, which are formed in the redshift interval $(z_c, z_c + dz_c)$ and survive till redshift z is (Sasaki 1994; Chiu & Ostriker 2000)

$$N(M, z, z_c) dM dz_c = \alpha N_M(z_c) \left(\frac{\delta_c}{D(z_c) \sigma(M)} \right)^2 \frac{\dot{D}(z_c)}{D(z)} \times \frac{dz_c}{H(z_c)(1+z_c)} dM. \quad (1)$$

Here the overdot represents time derivative, $N_M(z_c) dM$ is the number of collapsed objects per unit comoving volume within a mass range $(M, M + dM)$ at redshift z_c (Press & Schechter 1974). For greater accuracy, we have used Sheth & Tormen’s modified formula in the expression of $N_M(z_c) dM$ (Sheth & Tormen 1999), which fits the numerical simulations better than the original one, especially at high redshift. Here $\alpha = 0.707$ is a factor in Sheth & Tormen’s formula, δ_c is the critical over-density for collapse, usually taken to be 1.686 for a matter dominated flat universe ($\Omega_m = 1$). Note that this parameter is quite insensitive to the cosmology adopted and hence the same value can be used for all cosmological models (Eke et al. 1996). $H(z)$ is the Hubble parameter, $D(z)$ the growth factor for linear perturbations and $\sigma(M)$ the rms mass fluctuation at a mass scale M . In addition, $N(M, z, z_c)$ represents the formation rate of halos weighted by their survival probability, integrating it over z_c from z to ∞ gives the mass function $N_M(z)$ at any given redshift z : $N_M(z) = \int_z^\infty N(M, z, z_c) dz_c$, the original Sheth & Tormen’s PS formula.

In another direction, the formation and evolution of galaxies and the associated history of star formation have been studied extensively using both numerical simulations and semi-analytic models (Chiu & Ostriker 2000; Choudhury & Srianand 2002; Springel & Hernquist 2003; Nagamine et al. 2006). Following the previous work (e.g., Cen & Ostriker 1992; Chiu & Ostriker 2000; Choudhury & Srianand 2002), we assume that the SFR at z in a halo of mass M that has collapsed at an earlier redshift z_c is given by

$$\dot{M}_{\text{SF}}(M, z, z_c) = f_* M \frac{\Omega_b}{\Omega_m} \frac{t(z) - t(z_c)}{\kappa^2 t_{\text{dyn}}^2(z_c)} \exp\left(\frac{t(z) - t(z_c)}{-\kappa t_{\text{dyn}}(z_c)}\right). \quad (2)$$

¹ <http://www.stsci.edu/science/starburst99/>

Here f_* is the fraction of total baryonic mass in a halo that will be converted to stars. The values of f_* is between 0.1 (Barkana & Loeb 2001) and 0.2 (Choudhury & Ferrara 2006), while in this paper we set $f_* = 0.14$. The function $t(z)$ represents the age of the universe at redshift z . Thus, $t(z) - t(z_c)$ stands for the age of the collapsed halo at z . Given by Cen & Ostriker (1992), Chiu & Ostriker (2000) and Barkana & Loeb (2001), t_{dyn} is the dynamical time-scale. The duration of SF activity in a halo depends on the value of κ . Note that $\kappa \rightarrow 0$ corresponds to the SF occurring in a single burst. In this paper, we use the starburst model and take the value of κ to be 0.01².

Finally, the cosmic SFR per unit comoving volume (i.e. SFRD) at redshift z is

$$\dot{\rho}_{\text{SF}}^{\text{noFB}}(z) = \int_z^\infty dz_c \int_{M_{\text{low}}}^\infty N(M', z, z_c) dM' \dot{M}_{\text{SF}}(M', z, z_c), \quad (3)$$

where the lower mass cutoff M_{low} at a given epoch depends on the cooling efficiency of the gas and different feedback processes. We assign M_{low} a fixed value, $10^{10} M_\odot$, which means that the feedback effects of halos with mass below M_{low} are not considered.

2.2 AGN Feedback

The relationship between the formation rate of DM halos and the number density of super-massive black holes (SMBHs) has been revealed recently. This calls for a relation between the halo mass M and the BH mass M_{BH} (Lapi et al. 2006): $M_{\text{BH}} \approx 8 \times 10^6 \times (1+z)/7 \times (M/2.2 \times 10^{11} M_\odot)^{3.97}/[1 + (M/2.2 \times 10^{11} M_\odot)^{2.7}] M_\odot$. For simplicity, the growth time of the BH is ignored in this relationship. We consider a single-zone galaxy (a total gas mass M_{gas}) with three gas phases: diffuse gas in the outer regions, with mass M_{inf} infalling on a dynamical timescale, cool gas with mass M_{cold} , available to form stars, and hot gas with mass M_{hot} , eventually outflowing. Following Granato et al. (2004), the AGN feedback rate is

$$\dot{M}_{\text{cold}}^{\text{AGN}} \simeq 2 \times 10^3 \frac{M_{\text{cold}}}{M_{\text{gas}}} \frac{\epsilon_{\text{AGN}} (L_{\text{Edd}}/10^{46} \text{ erg s}^{-1})^{3/2}}{(\sigma/300 \text{ km s}^{-1})^2}. \quad (4)$$

Here L_{Edd} is the Eddington luminosity. The strength of AGN feedback $\epsilon_{\text{AGN}} = 1.3$ is recommended by Lapi et al. (2006). The $M_{\text{cold}}/M_{\text{gas}}$ in the right-hand side of Equation (4) is in the range $0.01 \leq M_{\text{cold}}/M_{\text{gas}} \leq 0.5$ (Granato et al. 2004; Lapi et al. 2006). For the line-of-sight velocity dispersion σ , we adopt the relationship $\sigma \simeq 0.65 V_c$ (Ferrarese 2002), where V_c is the circular velocity of the DM halo (Barkana & Loeb 2001).

2.3 SNe Feedback

Due to the feedback of SNe explosions, the gas in halos will be removed from the cold phase at the rate:

$$\dot{M}_{\text{cold}}^{\text{SN}} = \frac{2}{3} \dot{M}_{\text{SF}}(M, z, z_c) \epsilon_{\text{SN}} \frac{\eta_{\text{SN}} E_{\text{SN}}}{\sigma^2} = 0.42 \epsilon_{\text{SN}} \dot{M}_{\text{SF}}(M, z, z_c) \left(\frac{500 \text{ km s}^{-1}}{V_c} \right)^2, \quad (5)$$

where η_{SN} is the number of SNe expected per solar mass of formed stars (adopting a minimum progenitor mass of $8 M_\odot$). The ‘‘Starburst99’’ program for different IMF ($\alpha = 2.35, 3.3$) in an instantaneous starburst mode illustrates that η_{SN} is in range of $2 \times 10^{-4} \leq \eta_{\text{SN}} \leq 8 \times 10^{-3} M_\odot^{-1}$. Here we set $\eta_{\text{SN}} = 2.4 \times 10^{-3} M_\odot^{-1}$. E_{SN} is the kinetic energy of the ejecta from each supernova (10^{51} erg, e.g., Woosley & Weaver 1986), and ϵ_{SN} is the fraction of this energy used to reheat the cold gas. Some analyses show that about 90% of the SN kinetic energy may be lost by radiative cooling (Thornton et al. 1998; Heckman et al. 2000). We adopt $\epsilon_{\text{SN}} = 0.02, 0.04$ and 0.06 as our reference values.

² One can adopt other values 0.25, 0.5, 1.0 etc., but 0.01 fits the ‘‘Starburst99’’ result better.

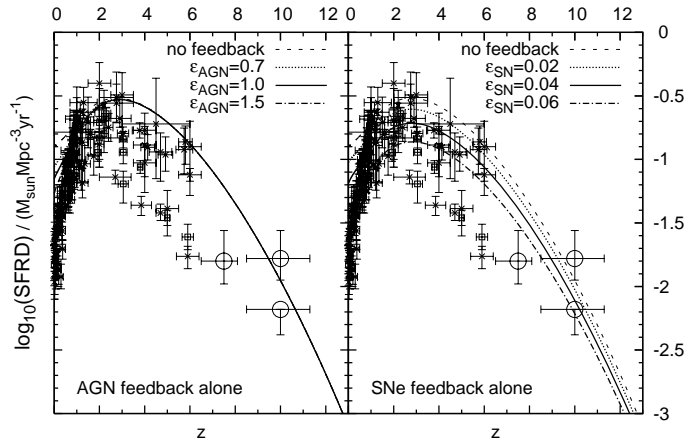


Fig. 1 AGN (left panel) and SNe (right panel) feedback. In the two panels, the dashed line is the SFRD without any feedback, while the other lines correspond to the different feedback parameters ϵ_{AGN} (ϵ_{SN}) shown in Table 1. The crosses are available in Hopkins & Beacom (2006), the squares come from Reddy et al. (2008), and the three circles are from the UDF (Bouwens et al. 2005).

Table 1 Three Cases of AGN and SNe Feedback Strength Factors

Feedback factors	Case A	Case B	Case C
ϵ_{AGN}	0.7	1.0	1.5
ϵ_{SN}	0.02	0.04	0.06

2.4 Feedback on SFRD

From Equations (5), (4) and (3), one can easily refresh the SFRD with AGN³ and SNe feedback:

$$\dot{\rho}_{\text{SF}}^{\text{FB}}(z) = \int_z^\infty dz_c \int_{M_{\text{low}}}^\infty dM' N \times \begin{cases} \dot{M}_{\text{SF}}^{\text{AGNFB}} & \text{(AGN feedback alone)} \\ \dot{M}_{\text{SF}}^{\text{SNFB}} & \text{(SNe feedback alone)} \\ \dot{M}_{\text{SF}}^{\text{TotFB}} & \text{(AGN + SNe feedbacks)} \end{cases}, \quad (6)$$

where $\dot{M}_{\text{SF}}^{\text{AGNFB}}$, $\dot{M}_{\text{SF}}^{\text{SNFB}}$ and $\dot{M}_{\text{SF}}^{\text{TotFB}}$ are described in Appendix A. We calculated the effects of the two feedback mechanisms on SFRD with the model parameters listed in Table 1. Figures 1 and 2 are the model output. On the left panel of Figure 1, only the AGN feedback is taken into account, while on the right one the SNe feedback is considered. In Figure 1, the dashed line is the SFRD without any feedback effect. The other lines correspond to different feedback parameters ϵ_{AGN} (or ϵ_{SN}) listed in Table 1. The crosses are taken from Hopkins & Beacom (2006). The squares come from Reddy et al. (2008), in which their multi-wavelength constraints on the global SFRD indicated that approximately one-third of the present-day stellar mass density was formed in sub-ultraluminous galaxies between redshifts $z = 1.9 \sim 3.4$. The three circles are from the UDF (Bouwens et al. 2005).

In Figure 1, we find an important difference between these two kinds of feedback: the AGN feedback takes effect only at low redshift ($z < 3$), while the SNe feedback affects SF in the whole SFH. In the AGN feedback cases, the lower the redshift, the stronger the feedback. A simple explanation is that AGN feedback depends on the central BH mass M which is associated with the halo mass, but the massive halos ($M \geq 10^{11} M_\odot$) appear abundantly only at low redshift according to the “bottom-up” hierarchical structure model (see Mo & White 2002 for details). In the SNe feedback cases, in general, the formation of stars in a galaxy is always accompanied by SNe events.

³ Here $\dot{M}_{\text{cold}}^{\text{AGN}}$ is a function of M' and z_c .

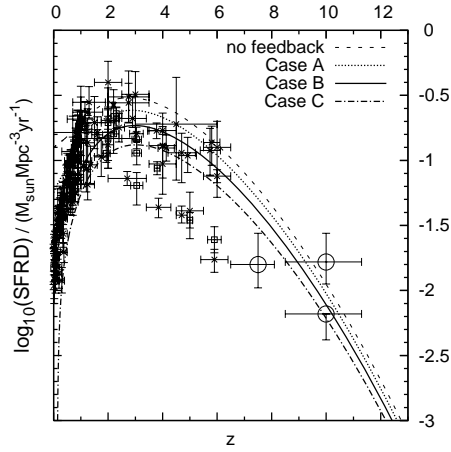


Fig. 2 Both the AGN and SNe feedbacks are included in the three cases labelled A, B and C in Table 1. The observed data points are the same as in Fig. 1. *Case C* contains the strongest feedback effects of both SNe and AGN and its curve drops sharply at the low redshift end.

However, as shown in Figure 1, the AGN feedback alone or the SNe feedback alone can not explain the observational data-points very well. The SFRD with AGN feedback only fails to fit the high redshift data, while the SNe feedback alone, the low redshift data. So we combined the two feedback mechanisms in the three cases listed in Table 1. The calculated results are shown in Figure 2. It is obvious that, of the cases, *Case B* (corresponding to the combination $\epsilon_{\text{AGN}} = 1.0$ and $\epsilon_{\text{SN}} = 0.04$) fits the observational data points best. About 92% of the observational data points are located between the curves of *Case A* and *Case C*. *Case C*, where both the SNe and AGN feedback effects are strongest, displays a sharp drop at the low redshift end.

3 THE NEAR-INFRARED BACKGROUND FROM STAR FORMATION GALAXIES

Excessive emission of the NIRB has been found in different observations (e.g., COBE, IRST and Spitzer) and in number counts of normal galaxies (Totani et al. 2001; Matsumoto et al. 2005). There have been many discussions on this topic in the past few years. Some authors alleged that the excess NIRB light component comes from the first luminous objects: Pop III massive stars (Salvatera et al. 2003; Dwek et al. 2005), since the spectral features of the excessive emission are very similar to that of the redshifted continuum and recombination line emission from HII regions generated by the first generation stars. However, other authors (Kashlinsky et al. 2005; Salvatera et al. 2006) found that Pop III stars contribute only $< 40\%$ of the total background intensity produced by all galaxies (hosting both Pop III and Pop II stars) at $z \geq 5$. Here, we calculate the effects of AGN and SNe feedback on the NIRB.

We use the code “Starburst99” to generate the template spectrum in units of $[\text{erg s}^{-1} \text{ \AA}^{-1} M_{\odot}^{-1}]$. We consider stars in the mass range $0.1M_{\odot} \leq m_{\text{stellar}} \leq 100M_{\odot}$ and use the Padova tracks for the AGB stars. We ran the program for two values of the IMF exponent, $\alpha = 2.35$ (Salpeter-type) and 3.3 (Miller & Scalo 1979) and three values of metallicity ($Z = 0.001, 0.008, 0.020$). We found a minor difference between $Z = 0.001$ and $Z = 0.020$ in the spectrum in the wavelengths $\lambda > 912 \text{ \AA}$, within 100 Myr after the starburst. We selected $Z = 0.008$ as our reference value for the metallicity.

3.1 NIR Flux and Comoving Specific Emissivity

The mean specific flux of the background light $\lambda_0 J(\lambda_0, z_0)$, seen at wavelength λ_0 by an observer at redshift z_0 , is given by

$$\lambda_0 J(\lambda_0, z_0) = \frac{\lambda_0}{4\pi} \int_{z_0}^{\infty} \Upsilon(\lambda, z) e^{-\tau_{\text{eff}}(\lambda_0, z_0, z)} \frac{ds}{dz} dz. \quad (7)$$

Table 2 Coefficients A_j Corresponding to λ_j in Eq. (10)

j	λ_j [Å]	A_j
2	1216	3.6×10^{-3}
3	1026	1.7×10^{-3}
4	973	1.2×10^{-3}
5	950	9.3×10^{-4}

$\tau_{\text{eff}}(\lambda_0, z_0, z)$ represents the effective optical depth at λ_0 of the IGM between redshift z_0 and z , and ds/dz stands for the proper line element.

The comoving specific emissivity, in units of $\text{erg s}^{-1} \text{Å}^{-1} \text{cm}^{-3}$, is

$$\Upsilon(\lambda, z) = l(\lambda, z) \frac{\int_0^{t_z} \dot{\rho}_{\text{SF}}^{\text{FB}}(t_{z'}) dt_{z'}}{\int_0^{t_z} \dot{\rho}_{\text{SF}}^{\text{noFB}}(t_{z'}) dt_{z'}} \times \int_{M_{\text{low}}}^{\infty} f_* M \frac{\Omega_b}{\Omega_m} N_M(z) dM, \quad (8)$$

where $l(\lambda, z)$ is the template specific luminosity of the population (in $\text{erg s}^{-1} \text{Å}^{-1} M_{\odot}^{-1}$) at redshift z , and t_z or t'_z is the age of the universe at z or z' (see Schneider et al. 2006 and Salvaterra & Ferrara 2003). M_{low} stands for the lower mass cutoff at a given epoch, the same one as in Equation (3).

3.2 Attenuation by the Medium in Space

We take three kinds of optical depth into account along the light propagation direction: (1) the absorption of the Lyman series lines and Lyman continuum by the intergalactic medium (mainly HI) τ_{IGM} ; (2) the extinction by the intergalactic dust τ_{IGD} ; (3) and the attenuation of the luminous galaxies by the interstellar medium (ISM), τ_{ISM} . This means the total effective optical depth is

$$\tau_{\text{eff}} = \tau_{\text{IGM}} + \tau_{\text{IGD}} + \tau_{\text{ISM}}. \quad (9)$$

Accordingly, the effective optical depth for the lines of the Lyman series ($912 \text{ Å} < \lambda_0/(1+z) < 1216 \text{ Å}$) which originates from the resonance absorption of HI atoms can be written as a sum (Madau 1995):

$$\tau_{\text{lines}} = \sum_{j=2,i} A_j \left(\frac{\lambda_0}{\lambda_j} \right)^{3.46}, \quad (10)$$

where λ_j and the corresponding values for A_j are given in Table 2.

Furthermore, for the Lyman continuum absorption ($\lambda_0/(1+z) \leq 912 \text{ Å}$) by Poisson distributed absorbers (Madau 1991; Madau 1992) the effective optical depth reads

$$\tau_{\text{conti}} = \int_{z_0}^z dz' \int_0^{\infty} dN_{\text{HI}} \zeta(N_{\text{HI}}, z') \left(1 - e^{-\tau(N_{\text{HI}}, \lambda_0, z')} \right), \quad (11)$$

where $\zeta(N_{\text{HI}}, z') = d^2N/dN_{\text{HI}} dz'$ is the distribution of the absorbers as a function of the redshift and neutral hydrogen column density, N_{HI} . $\tau(N_{\text{HI}}, \lambda_0, z') = N_{\text{HI}} \sigma$ stands for the optical depth of an individual cloud for ionizing radiation at wavelength $\lambda_0/(1+z')$. Here $\sigma(\lambda_0, z') \sim 6.3 \times 10^{-18} (\lambda_0/912 \text{ Å})^3 (1+z')^{-3} \text{ cm}^2$ (Osterbrock 1989) is the hydrogen photoionization cross section. For the redshift and column density distribution of the absorption lines, the usual form can be adopted:

$$\zeta(N_{\text{HI}}, z) = \left(\frac{A}{10^{17}} \right) \left(\frac{N_{\text{HI}}}{10^{17} \text{ cm}^{-2}} \right)^{-\beta} (1+z)^{\gamma}, \quad (12)$$

where the values of the coefficients A , β and γ in different ranges in N_{HI} , taken from Fardal, Giroux & Shull (1998), are given in Table 3.

At last, we obtain the effective optical depth τ_{IGM} in the emitter rest frame at wavelength $\lambda_0/(1+z) < 1216 \text{ Å}$:

$$\tau_{\text{IGM}} = \begin{cases} \tau_{\text{conti}}; & \lambda_0/(1+z) \leq 912 \text{ Å} \\ \tau_{\text{lines}}; & 912 \text{ Å} < \lambda_0/(1+z) < 1216 \text{ Å} \end{cases}. \quad (13)$$

Table 3 Best fit values of A , β and γ in Eq. (12) (Fardal et al. 1998)

N_{HI}	A	β	γ
$< 10^{14}$	1.45×10^{-1}	1.40	2.58
$10^{14} - 10^{16}$	6.04×10^{-3}	1.86	2.58
$10^{16} - 10^{19}$	2.58×10^{-2}	1.23	2.58
$10^{19} - 10^{22}$	8.42×10^{-2}	1.16	1.30

When the first generation massive stars died out in SNe explosions, the ISM and IGM were enriched by metals (in dust) which are usually carried everywhere by the SN winds. The graphite and silicate grains can attenuate the light by scattering and absorbing photons (the so-called extinction). For the IGD extinction case, following Inoue et al. (2004) and Corasaniti (2006), the amount of the IGD extinction is given by

$$\tau_{\text{IGD}} = \frac{3c\Omega_b\rho_{c,0}}{4a\rho} \int_0^z Q\left(a, \frac{\lambda_0}{1+z'}\right) \frac{\mathcal{D}^{\text{IGM}}(z')dz'}{H(z')(1+z')^{-2}}, \quad (14)$$

where a is the grain radius, $\rho_{c,0}$ is the critical density of the current universe, c is the light speed, and $\rho (= 2 \text{ g cm}^{-3})$ is the grain material density. For simplicity, we have assumed that the dust grains follow a uniform distribution with no structure. Q is the extinction efficiency factor, evaluated by the Mie code (from the Lorenz-Mie scattering theory) or the DDA code (from the Discrete Dipole Approximation method, see Draine 2004). We deduce Equation (14) by combining equations (3), (4) and (5) in Inoue et al. (2004). Bohren and Huffmann's BHMIE code is used to calculate the extinction efficiency factor Q . In Equation (14), $\mathcal{D}^{\text{IGM}}(z)$ is the dust-to-gas mass ratio in the IGM.

As for the case of ISM extinction, with the same origin of attenuation as the IGD, we obtain a useful formula from Charlot & Fall (2000) and Kong et al. (2004): the 'effective absorption' curve describing the attenuation of photons emitted in all directions by stars in a galaxy:

$$\tau_{\text{ISM}} = \hat{\tau}_{\text{V}} \left(\frac{\lambda_0/(1+z)}{5500 \text{ \AA}} \right)^{-0.7}, \quad (15)$$

where $\hat{\tau}_{\text{V}}$ is the total effective V -band optical depth with a fixed value $\hat{\tau}_{\text{V}} = 1.5$ in our model.

3.3 The Emission Spectra and NIR Flux

When light leaves a distant galaxy, passes through ISM, IGM, IGD and eventually arrives at the earth, its spectra will be redshifted and reddened. Moreover, the emission flux is related to the evolutionary time of the sources. This means that for the same starburst galaxy at different times, we will receive different spectra. Here we compare four spectra⁴, emitted at $4 \times 10^7 \text{ yr}$, $8 \times 10^7 \text{ yr}$, $1.2 \times 10^8 \text{ yr}$ and $2 \times 10^8 \text{ yr}$, respectively, from an instantaneous starburst. The Salpeter IMF (with $0.1 M_{\odot} \leq m_{\text{stellar}} \leq 100 M_{\odot}$) and a $Z = 0.008$ metallicity were taken as our initial conditions when we ran "Starburst99" to acquire the template specific luminosity $l(\lambda, z)$.

The calculated results of Equation (7) are shown in Figure 3. The four curves in each panel represent the case of no feedback and the three feedback cases as listed in Table 1. Figure 3 also shows recent measurements of the extragalactic near-infrared/optical background based on IRTS (filled squares, Matsumoto et al. 2005), HST (filled triangles, Bernstein et al. 2002a), and integrated optical galaxy number counts (filled diamonds, Totani et al. 2001). From Figure 3, we obtain the following conclusions: (1) The observed emission flux is mainly from the starburst galaxies at an age between $\sim 10^7 \text{ yr}$ and $\sim 10^8 \text{ yr}$, and from the second and third panels, about 70%–80% IRTS points are located in the area between *Case A* and *Case C*. (2) Feedback is important for the NIRB flux. In these four panels we can see obviously that the NIRB flux in the no-feedback case is always larger than in the with-feedback cases. (3) None of the cases considered can fit the IRTS data points in the range 13000–22000 Å, at the peak flux. Perhaps, this indicates that the massive Pop III stars which exist before $z > 10$ can give a possible explanation of this discrepancy.

⁴ These spectra are available in "Starburst99" code on the website <http://www.stsci.edu/science/starburst99/>.

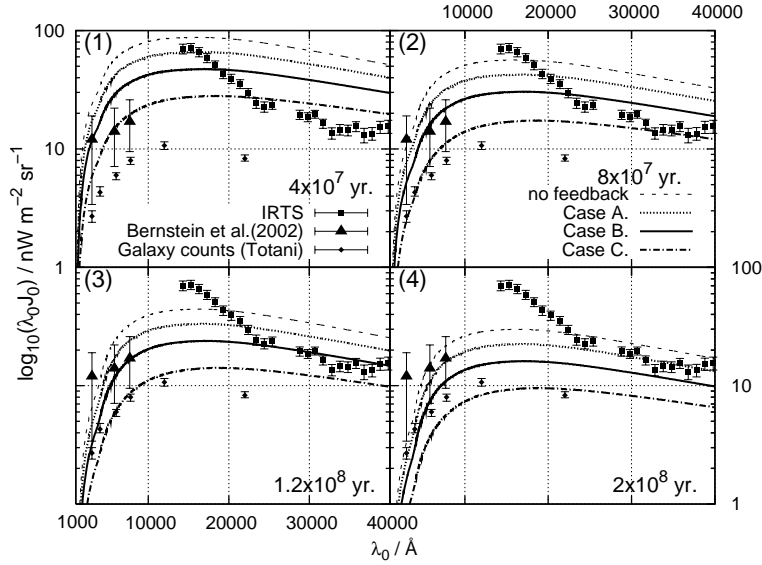


Fig. 3 Spectra emitted at different times in starburst galaxies. A $Z = 0.008$ metallicity and the Salpeter IMF ($\alpha = 2.35$) were used to plot the four set of lines. The observed data are based on IRTS (the filled squares, Matsumoto et al. 2005), HST (the filled triangles, Bernstein et al. 2002a), and integrated optical galaxy number counts (filled diamonds, Totani et al. 2001).

4 COSMOLOGICAL REIONIZATION

Cosmological reionization is an important process which puts tight constraints on the cosmological evolution of luminous objects. We check the relationship between the feedback effects and the history of cosmological reionization.

First, we assume that all the Lyman continuum photons escape from star forming galaxies are used to reionize the IGM and the photons emitted from the sources immediately join the action with the atom, regardless of the photon propagation between the source and the atom. The fraction of ionized hydrogen, Q_{HII} (the so-called filling factor), evolves as (Barkana & Loeb 2001)

$$\frac{dQ_{\text{HII}}}{dz} = \frac{\dot{N}_{\gamma}}{n_{\text{H}}(z)} \frac{dt}{dz} - \alpha_{\text{B}} n_{\text{H}}(z) Q_{\text{HII}} C \frac{dt}{dz}. \quad (16)$$

Here \dot{N}_{γ} is the rate of UV photons escaping into the IGM, $n_{\text{H}}(z)$ stands for the proper number density of the hydrogen atoms. The volume averaged clumping factor of the IGM, C , is defined as $C \equiv \langle n_{\text{H}}^2 \rangle / \bar{n}_{\text{H}}^2$ and $\alpha_{\text{B}} = 1.13 \times 10^{-13} \text{ cm}^3 \text{ s}^{-1}$ is the *case B* recombination coefficient at $T \simeq 3 \times 10^4 \text{ K}$ (Seager et al. 1999). The first term on the right of Equation (16) is the rate of ionization and the second term is the rate of recombination weighted by the Q_{HII} , as the recombination takes place only in the ionized region. \dot{N}_{γ} is obtained from the SFRD calculation,

$$\dot{N}_{\gamma} = \frac{\dot{\rho}_{\text{SF}}(z)(1+z)^3}{m_{\text{p}}} n_{\gamma} f_{\text{esc}}. \quad (17)$$

Here n_{γ} is the number of ionizing photons released per baryon of stars formed, f_{esc} represents the fraction of photons that escape from the star forming halo, and $f_{\text{esc}} = 0.3$ is used in this model, following the suggestion of Mao et al. (2007); $\dot{\rho}_{\text{SF}}(z)$ is expressed in Equations (3) and (6). The value of n_{γ} depends on the IMF of the forming stars. For a Salpeter IMF (with $0.1 M_{\odot} \leq m_{\text{stellar}} \leq 100 M_{\odot}$), n_{γ} is about 4,000, evaluated by ‘‘Starburst99’’ with metallicity $Z = 0.008$. For the clumping factor C , we use the simple form given by Haiman & Bryan (2006).

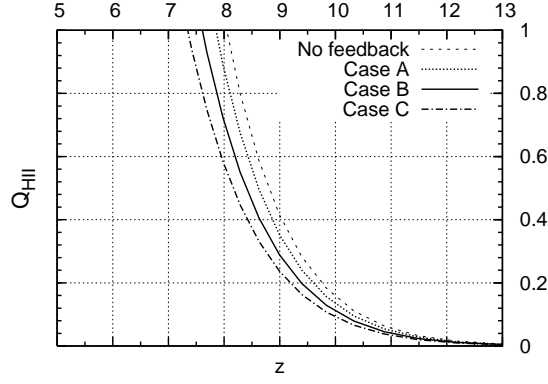


Fig. 4 Reionization history in four feedback cases. The four types of line have the same meaning as in Fig. 2.

Our results are plotted in Figure 4. We notice an important point, namely, the feedback can delay the completion of the neutral HI reionization. We conclude: (1) Our result of the reionization epoch is within the range by the *WMAP* observation ($7 \leq z_{\text{re}} \leq 12$), although Samui et al. (2007) argued that if Pop III stars or molecular cooling dominated halos are involved, the calculated result fits the *WMAP* data very well ($z_{\text{re}} \simeq 11$). (2) Due to $z_{\text{re}} = 7 \sim 8 > 3$, we find that SNe feedback should be responsible for the differences among the cases in Figure 4 (see Fig. 1 for the reason), which means the AGN feedback can hardly affect the reionization history. (3) Figure 4 implies a rapid growth of fraction of the HII region at $7 \leq z_{\text{re}} \leq 9$ ⁵. Since the reionization process is not a slow variation, we can not make a clean sweep of the uncertainties in the cosmological reionization history yet.

5 DISCUSSION

We overlooked some effects from the model parameters and treated them as definitely known quantities when we focused on the AGN and SNe feedback. Here we show the effects on our result from those parameters.

1. In Equation (3), f_* provides a choice to avoid the complicated problem of how baryons turned into stars. In this model, tuning f_* can not affect the relative strength (or relative ratio) of kinetic feedback (AGN and/or SNe), but the SFRD, Q_{HII} and the flux of NIRB will be changed. A higher value of f_* can lead to a higher SFRD, NIRB and earlier reionization epoch.
2. $M_{\text{cold}}/M_{\text{gas}}$ (in Eq. (4)) covers a large interval. It depends on many factors, e.g., the gas cooling rate, gas components and radiative feedback, etc. The AGN feedback will be enhanced if $M_{\text{cold}}/M_{\text{gas}}$ increases. So a higher cooling rate can result in a stronger feedback effect. We set $M_{\text{cold}}/M_{\text{gas}} \simeq 0.08$ for the halos of age $10^7 - 10^{8.5}$ yr (Granato et al. 2004; Lapi et al. 2006).
3. E_{SN} (in Eq. (5)) can reflect the explosion type of SNe. Roughly, a high E_{SN} stands for Type II SNe, the massive stars explosions. $E_{\text{SN}} = 10^{50}$ or 10^{52} erg corresponds to a lower or higher feedback effect from SNe. For simplicity, we adopted a representative value, 10^{50} erg, instead of computing the other cases.
4. In the ISM attenuation, $\hat{\tau}_V$ was set in the range $0.5 \leq \hat{\tau}_V \leq 2.0$, as suggested by Kong et al. (2004). Certainly, the NIRB will be increased if the value of $\hat{\tau}_V$ is reduced, because more *UV* or *V*-band photons can then escape from the galaxies.

Other parameters in this model are mostly from numerical simulations or fittings to observational data, e.g., the α (in Eq. (1)) and A , β , γ in Table 3. In these cases, the values favoured by the authors are adopted in this work.

⁵ Fan et al. (2006) found there is a rapid increase in the neutral fraction of the IGM nearby $z \simeq 6$, less than 50% at $z \sim 6.5$.

6 CONCLUSIONS

By modeling the feedback effects of AGN and SNe, we obtained some results regarding the SFH, cosmological reionization and NIRB. Besides the neutral hydrogen dominated IGM attenuation (already considered by Salvaterra et al. 2003, 2006), we introduced the ISM and IGD attenuations in our calculation of the NIRB flux. This consideration is reasonable and can help recover the real physical conditions of the medium in the universe. We also found that the NIRB could be very sensitive to the IMF and metallicity. We now present our main conclusions as follows:

1. The AGN and SNe feedback effects on SFH are different. The AGN feedback is effective at low redshifts, while the SNe feedback affects the whole SFH.
2. The NIRB flux decreases as the feedback strength increases, and the flux approaches a constant value in the range (8000 ~ 40000 Å). The failure of fitting the peak shaped IRTS points in the band 13 000~22 000 Å, may imply the existence of massive Pop III stars at very high redshifts.
3. With the SN kinetic feedback the reionization epoch has a more extended redshift range, compared to the case of no feedback. The feedback appears able to postpone to bring the neutral HI reionization to completion.

Our analytic model failed to explain part of the IRTS data points. The contribution of Pop III stars to the peak around 13 000~22 000 Å will be examined in a future work.

Acknowledgements We thank X. Kong for advice on the calculation of τ_{eff} , and Andrew Hopkins and Naveen Reddy for kindly providing the data on SFRD. The code “Starburst99” helped us realize our analytic model, especially in the calculation of η_{SN} and the stars spectra. We also thank “Starburst99” group for providing the galaxies spectra.

Appendix A: THE SFR WITH SN AND AGN FEEDBACK

In Cen & Ostriker (1992), equation (2) is just an assumption. In fact, one can obtain the relation from more simple assumption and proper deduction. Following Cen & Ostriker (1992), in a halo of mass M , the baryonic gas has mass of $M_b(0) = \frac{\Omega_b}{\Omega_m} \times M$ initially. After Δt , some baryonic gas condensed to cold gas M_{cold} (the so-called collisionless particles in Cen & Ostriker 1992). Then we have

$$\Delta M_b = -M_b(0)\Delta t/t_{\text{dyn}} \quad \text{and} \quad \Delta M_{\text{cold}} = +M_b(0)\Delta t/t_{\text{dyn}}, \quad (\text{A.1})$$

where t_{dyn} is the free-fall time or dynamical time-scale (hereafter we reduced t/t_{dyn} to t except for special noticing). We draw a conclusion from Equation (A.1) that ΔM_b and ΔM_{cold} are all directly proportional to $M_b(t)$ at time t . This is an implicit assumption in Cen & Ostriker (1992). When $\Delta t \rightarrow dt$ we read

$$dM_b(t) = -M_b(t)dt \quad \text{and} \quad dM_{\text{cold}}(t) = +M_b(t)dt. \quad (\text{A.2})$$

By solving Equation (A.2) with initial condition Equation (A.1), we obtain

$$M_b(t) = M_b(0) \exp(-t) \quad \text{and} \quad M_{\text{cold}}(t) = \int_0^t M_b(t')dt' = M_b(0) [1 - \exp(-t)]. \quad (\text{A.3})$$

Cold gas can form stars in the efficiency f_* . We assume that the newly formed star mass per unit time, \dot{M}_{SF} , is proportional to the net mass of cold gas at that time, $M_{\text{cold}}^{\text{net}}(t)$,

$$\dot{M}_{\text{SF}}(t) = f_* \times M_{\text{cold}}^{\text{net}}(t), \quad (\text{A.4})$$

where

$$M_{\text{cold}}^{\text{net}}(t) = M_{\text{cold}}(t) - f_*^{-1} \int_0^t \dot{M}_{\text{SF}}(t')dt'. \quad (\text{A.5})$$

Solving Equation (A.4) with $\dot{M}_{\text{SF}}(0) = 0$ ($M_{\text{cold}}^{\text{net}}(0) = 0$), we have

$$dM_{\text{SF}}(t) = f_* M_b(0) \times t \exp(-t) dt. \quad (\text{A.6})$$

If we replace t with $[t(z) - t(z_c)] / [\kappa t_{\text{dyn}}(z_c)]$ (here $t(z)$ is variable), we obtain Equation (2). Since the feedback of SNe explosions removing the cold gas at the rate $\dot{M}_{\text{cold}}^{\text{SN}} = 1.1 \epsilon_{\text{SN}} \dot{M}_{\text{SF}}(t) \left(\frac{500 \text{ km s}^{-1}}{V_c} \right)^2$, we have

$$\begin{aligned} M_{\text{cold}}^{\text{net}}(t) &= M_{\text{cold}}(t) - f_*^{-1} \int_0^t \dot{M}_{\text{SF}}(t') dt' - \int_0^t \dot{M}_{\text{cold}}^{\text{SN}}(t') dt' \\ &= M_{\text{cold}}(t) - \int_0^t \left[f_*^{-1} + 1.1 \epsilon_{\text{SN}} \left(\frac{500}{V_c} \right)^2 \right] \dot{M}_{\text{SF}}(t') dt', \end{aligned} \quad (\text{A.7})$$

where the circular velocity V_c is a function with two variables M and z (Barkana & Loeb 2001). $\left\{ \frac{\Omega_m}{\Omega_m(z)} \frac{\Delta_c(z)}{18\pi^2} \right\}^{1/3}$ varies between 0.65 and 1.0 when z is from 30 to zero. For simplicity we use an intermediate value 0.75 in this work:

$$V_c(M, z_c) = \sqrt{0.75} \times 23.4 \left(\frac{M}{10^8 h^{-1} M_\odot} \right)^{1/3} \left(\frac{1+z_c}{10} \right)^{1/2}. \quad (\text{A.8})$$

Solving Equation (A.4) again with $\dot{M}_{\text{SF}}(0) = 0$, we then have the SFR with SNe feedback:

$$dM_{\text{SF}}^{\text{SNFB}}(t) = \frac{M_b(0)}{S(M, z_c)} \left\{ \exp(-t) - \exp \left\{ - \left[f_* S(M, z_c) + 1 \right] t \right\} \right\} dt, \quad (\text{A.9})$$

where $S(M, z_c) = 1.82 \times 10^9 \epsilon_{\text{SN}} M^{-2/3} (1+z_c)^{-1}$ is a function of halo mass and the halo formed time. Substituting $[t(z) - t(z_c)] / [\kappa t_{\text{dyn}}(z_c)]$ for t , we have the SFR with SNe feedback:

$$\dot{M}_{\text{SF}}^{\text{SNFB}}(M, z, z_c) = \frac{\Omega_b M}{\Omega_m S(M, z_c) \kappa t_{\text{dyn}}} \left\{ \exp \left[- \frac{t(z) - t(z_c)}{\kappa t_{\text{dyn}}(z_c)} \right] - \exp \left\{ - \left[f_* S(M, z_c) + 1 \right] \frac{t(z) - t(z_c)}{\kappa t_{\text{dyn}}(z_c)} \right\} \right\}. \quad (\text{A.10})$$

Obviously, Equation (A.10) will return to Equation (2) when $S_{\text{III}}(M, z_c)$ approaches zero.

Unfortunately, for the AGN feedback case we can not obtain an analytical solution. Following the case of SNe feedback, we have

$$M_{\text{cold}}^{\text{net}}(t) = M_{\text{cold}}(t) - f_*^{-1} \int_0^t \dot{M}_{\text{SF}}(t') dt' - \int_0^t \dot{M}_{\text{cold}}^{\text{AGN}}(t') dt', \quad (\text{A.11})$$

Solving Equation (A.4) numerically with initial condition $\dot{M}_{\text{SF}}(0) = 0$, we obtain the SFR with AGN feedback $\dot{M}_{\text{SF}}^{\text{AGNFB}}(M, z, z_c)$.

Finally, by solving Equation (A.4) with the following equation:

$$M_{\text{cold}}^{\text{net}}(t) = M_{\text{cold}}(t) - f_*^{-1} \int_0^t \dot{M}_{\text{SF}}(t') dt' - \int_0^t \dot{M}_{\text{cold}}^{\text{AGN}}(t') dt' - \int_0^t \dot{M}_{\text{cold}}^{\text{SN}}(t') dt', \quad (\text{A.12})$$

we obtain the SFR accompanied by AGN and SNe feedback $\dot{M}_{\text{SF}}^{\text{TotFB}}(M, z, z_c)$.

References

- Barkana R., Loeb A., 2001, *PhR*, 349, 125
- Bernstein R. A., Freedman W. L., Madore B. F., 2002a, *ApJ*, 571, 56
- Bouwens R. J., Illingworth G. D., Thompson R. I., Franx M., 2005, *ApJ*, 624, L5
- Bouwens R. J., Illingworth G. D., Blakeslee J. P., Franx M., 2006, *ApJ*, 653, 53
- Cen R., Ostriker P., 1992, *ApJ*, L339, 113
- Charlot S., Fall M., 2000, *ApJ*, 539, 718
- Chiu W. A., Ostriker J. P., 2000, *ApJ*, 534, 507
- Choudhury T. R., Srianand R., 2002, *MNRAS*, 336, L27
- Choudhury T. R., Ferrara A., 2006, *MNRAS*, 371, L55
- Corasaniti P. S., 2006, *MNRAS*, 372, 191
- Draine B. T., Flatau P. J., 2004, [arXiv:astro-ph/0409262](https://arxiv.org/abs/astro-ph/0409262)
- Dwek E., Arendt R. G., Krennrich F., 2005, *ApJ*, 635, 784
- Eke V. R., Cole S., Frenk C. S., 1996, *MNRAS*, 282, 263
- Fan X., Strauss M. A., Richards G. T. et al., 2006, *AJ*, 131, 1203
- Fardal M. A., Giroux M. L., Shull J. M., 1998, *AJ*, 115, 2206
- Ferrarese L., 2002, *ApJ*, 578, 90
- Granato G., De Zotti G., Silva L. et al., 2004, *ApJ*, 600, 580
- Gunn J. E., Peterson B. A., 1965, *ApJ*, 142, 1633
- Heckman T. M., Lehnert M. D., Strickland D. K., Armus L., 2000, *ApJS*, 129, 493
- Haiman Z., Bryan G., 2006, *ApJ*, 650, 7
- Hopkins A., Beacom J., 2006, *ApJ*, 651, 142
- Inoue A. K., Kamaya H., 2004, *MNRAS*, 350, 729
- Kashlinsky A., Arendt R. G., Mather J., Moseley S. H., 2005, *Nature*, 438, 45
- Kong X., Charlot S., Brinchmann J., Fall S. M., 2004, *MNRAS*, 349, 769
- Lapi A., Shankar F., Mao J. et al., 2006, *ApJ*, 650, 42
- Loeb A., Peebles P. J. E., 2003, *ApJ*, 589, 29
- Madau P., 1991, *ApJ*, 376, L33
- Madau P., 1992, *ApJ*, 389, L1
- Madau P., 1995, *ApJ*, 441, 18
- Mao J., Lapi A., Granato G. L., de Zotti G., Danese L., 2007 *ApJ*, 667, 655
- Matsumoto T. et al., 2005, *ApJ*, 626, 31
- Miller G. E., Scalzo J. M., 1979, *ApJS*, 41, 513
- Mo H. J., White S. D. M., 2002, *MNRAS*, 336, 112
- Nagamine K., Ostriker J. P., Fukugita M., Cen R., 2006, *ApJ*, 653, 881
- Osterbrock D. E., 1989, *Astrophysics of Gaseous Nebulae and Active Galactic Nuclei*, Mill Valley: University Science Book
- Peebles P. J. E., 1993, *Principles of Physical Cosmology*, Princeton Univ. Press, Princeton, NJ
- Press W. H., Schechter P., 1974, *ApJ*, 187, 425
- Reddy N. A., Steidel C. C., Pettini M. et al., 2008, *ApJS*, 175, 48
- Salvaterra R., Ferrara A., 2003, *MNRAS*, 339, 973
- Salvaterra R., Magliocchetti M., Ferrara A., Schneider R., 2006, *MNRAS*, L368
- Samui S., Srianand R., Subramanian K., 2007, *MNRAS*, 377, 285
- Sasaki S., 1994, *PASJ*, 46, 427
- Schneider R., Salvaterra R., Ferrara A., Ciardi B., 2006, *MNRAS*, 369, 825
- Seager S., Sasselov D. D., Scott D., 1999, *ApJ*, 523, L1
- Sheth R. K., Tormen G., 1999, *MNRAS*, 308, 119
- Spergel D. N., Bean R., Dore O. et al., 2007, *ApJS*, 170, 377
- Springel V., Hernquist L., 2003, *MNRAS*, 339, 289
- Thornton K., Gaudlitz M., Janka H. T., Steinmetz M., 1998, *ApJ*, 500, 95
- Totani T., Yoshii Y., Iwamuro F. et al., 2001, *ApJ*, L550, 137
- White S. D. M., Rees M., 1978, *MNRAS*, 183, 341
- Woosley S. E., Weaver T. A., 1986, *ARA&A*, 24, 205
- Wyithe J. S. B., Loeb A., Carilli C., 2005, *ApJ*, 628, 575